Article

Validating clear air absorption models using ground-based microwave radiometers and vice-versa

TIM HEWISON[1*], DOMENICO CIMINI[2], LORENZ MARTIN[3], CATHERINE GAFFARD[1] AND JOHN NASH[1]

[1] Met Office, University of Reading, UK
[2] IMAA, National Research Council, Italy and CIRES, University of Colorado at Boulder, USA
[3] Institute of Applied Physics, University of Bern, Switzerland

Abstract

Microwave radiometer observations are compared with various radiative transfer model calculations based on simultaneous radiosondes. This analysis uses observations from Payerne, Switzerland, in cloud free conditions during the Temperature Humidity and Cloud (TUC) experiment in winter 2003/04. The results show a systematic bias in the brightness temperatures measured by the Radiometrics profiler at 55 – 59 GHz, which has since been corrected in the control software. Observations at lower frequencies (22 – 30 GHz) in these cold conditions do not support recent proposed changes to the width of the 22.235 GHz water vapour line, although this is subject to the assumption of no residual bias in the radiosonde humidity. At intermediate frequencies (51 – 54 GHz), the absorption models produce large differences, which may be due to differences in oxygen line coupling and highlight the need for further laboratory measurements at low temperatures.

Zusammenfassung

Bodengestützte Mikrowellen-Radiometer Messungen der troposphärischen Helligkeitstemperatur werden mit Strahlungstransfer-Berechnungen verglichen, die auf gleichzeitigen Radiosondierungen beruhen. Im Vergleich werden Daten der Temperature Humidity and Cloud (TUC) Kampagne verwendet, die im Winter 2003/04 in Payerne, Schweiz, gewonnen wurden. Die Resultate zeigen systematische Fehler in den Helligkeitstemperaturen des Profilers von Radiometrics zwischen 55 und 59 GHz, die in der weiteren Datenverarbeitung berücksichtigt wurden. Im Gegensatz zu aktuellen Vorschlägen zeigen die Messungen zwischen 22 und 30 GHz bei tiefen Lufttemperaturen keinen Bedarf einer Änderung der Breite der Wasserdampf-Absorptionslinie bei 22.235 GHz. Zwischen 51 und 54 GHz gibt es grosse Unterschiede zwischen den geprüften Modellen, was mit Unterschieden in der Kopplung der Sauerstoff-Linien erklärt werden kann. Die Unterschiede legen weitere Labormessungen bei tiefen Temperaturen nahe.

1. Introduction

Microwave radiometer observations can be used to retrieve information on the profiles of temperature, humidity and cloud in the troposphere. Although these retrievals can apply various techniques (CIMINI et al., 2006a), most are sensitive to biases in a microwave radiometer's observations and the absorption model used in the radiative transfer calculations. Therefore, it is important to understand these biases in order to improve the instruments, absorption models and, ultimately, the retrievals.

This paper compares coincident measurements from MeteoLabor SRS400 radiosondes (RUFFIEUX et al., 2006) and two microwave radiometers: ASMUWARA (MARTIN et al., 2006a) and a Radiometrics TP/WVP-3000 (WARE et al.., 2003) in brightness temperature (T_b) space. This is done using radiative transfer calcu-

lations with different absorption models, described in section 2. This provides an independent validation of both the radiometer observations and the absorption models. However, it is not possible to distinguish biases from each source without reference to an error analysis. During the TUC experiment, we have the additional advantage of coincident measurements from two microwave radiometers to assist in this discrimination. CIMINI et al. (2006b) compare observations from similar channels to these radiometers. Their results provide additional confidence in the conclusions.

2. Absorption Models used in this study

2.1. MPM87 (LIEBE and LAYTON, 1987)

The clear air absorption part of the Millimeter-wave Propagation Model, MPM87 includes 30 water vapour lines and 44 oxygen lines all in the range 20 GHz –

---

[*] Corresponding Author: Tim Hewison, Met Office, Meteorology Building, PO Box 243, Earley Gate, University of Reading, RG6 6BB, UK, mailto:tim.hewison@metoffice.gov.uk, phone: +44 118 3787830, fax: +44 118 3788791

1 THz, based on theoretical values and a Van-Vleck Weisskopf shape function. These are supplemented by an empirically derived water vapour continuum, fitted to laboratory observations at 138 GHz. However, these observations were limited to 282 – 316 K, and must be extrapolated for typical atmospheric conditions. Additional terms represent the non-resonant absorption due to the Debye spectrum of oxygen below 10 GHz and the pressure-induced nitrogen absorption above 100 GHz, which can become a significant contribution to the overall absorption in low humidity.

2.2. MPM89 (LIEBE, 1989)

The 1989 revision of MPM modified the parameters describing the 22 and 183 GHz water vapour lines, fitting the pressure broadened line width with four parameters, instead of one. Other components are the same as MPM87 for the purposes of this study.

2.3. MPM93 (LIEBE et al, 1993)

This version of MPM, has 34 water vapour lines between 20 – 1000 GHz, defined in a slightly different manner from MPM89. The 183 GHz line is 8.5% wider and 5% stronger than in MPM89. The water vapour continuum absorption is formulated as a "pseudo-line" near 2 THz, and has a different temperature dependence, based on newer observations. Like its predecessors, MPM93 includes 44 oxygen lines with the same line strengths, but 5% greater widths and 15% stronger mixing than MPM89. The non-resonant nitrogen absorption is essentially the same as MPM89 at the frequencies in this study.

2.4. Ros98 (ROSENKRANZ, 1998)

Ros98 uses 15 water vapour line parameters, which are very similar to the strongest lines used in MPM89. The other half of the lines have been omitted as they were judged to have negligible impact. Rosenkranz's investigations suggested a range of observations could be best modelled by using a water vapour continuum with a combination of MPM87's foreign-broadened component, and MPM93's self-broadened component. However, the water vapour lines used were truncated at ±750 GHz, so the foreign- and self- broadened parts of the water vapour continuum were increased 15% and 3%, respectively to compensate. This model uses the same oxygen line parameters as MPM93, except at sub-millimetre frequencies, where values from the HITRAN database were used. It also uses a different form of non-resonant absorption due to pressure broadening by nitrogen.

2.5. Ros03 (Personal communication)

In 2003 Rosenkranz updated his water vapour model to include recent measurements and pressure line shift mechanism (LILJEGREN et al., 2005). He also corrected some line intensities and revised the width of the 425 GHz oxygen line and the mixing and width of the 118.75 GHz line and adopted recent sub-millimetre observations suggesting the strength of the dry nitrogen absorption should be increased by 29%. The intensity and air-broadened width of the 183 GHz line are 0.264% and 2% higher in Ros03 than Ros98. Other parameters of this line are unchanged.

The zenith T_bs modelled with Ros98 and Ros03 are within 0.06 K for all the channels used in the TUC dataset, except 151 GHz. So this model will not be discussed further in its own right.

2.6. Lil05 (LILJEGREN et al., 2005)

LILJEGREN et al. (2005) used a model based on Ros03, but with a 5% smaller width of the 22 GHz line. They also suggested replacing the Ros03 continuum with MT_CKD (MLAWER et al., 2003). These modifications were based on comparisons of zenith T_b modelled and observed with a radiometer similar to one used in this study. They showed the modifications improved the fit with observed T_b trends, and also reduced the errors in profiles retrieved from them.

3. Previous work

Several authors have attempted to use ground-based microwave radiometers and co-located radiosondes to check the validity of absorption models. As our error analysis shows, the confidence in the results depends on the accuracy of the radiometer and radiosonde calibration as well as the atmospheric variability. The conclusions will not generally be applicable to a broad range of atmospherics conditions, as the emission is predominately from the lower troposphere.

HEWISON et al. (2003) presented an independent validation of the performance of a microwave radiometer. T_bs observed in 12 channels from 22 – 59 GHz were compared with radiative transfer models, based on coincident radiosonde profiles in clear sky conditions. Biases were identified in the radiometer's 55 – 59 GHz channels, which caused biases in the retrieved temperature profile. Biases were also found in the water vapour channels around 23 GHz, partly due to a dry bias in the RS80H radiosonde.

CIMINI et al.(2004) conducted a similar analysis on data from 4 radiometers with a total of 19 channels between 20 – 59 GHz. They found that of these models Ros98 gave the best results at 20.6 – 20.7 GHz channels, while MPM93 was preferable close to 22.2 GHz. These 2 models stayed within 0.3 K at 23.8 GHz, but

Ros98 gave the best results in the atmospheric window (~30 GHz). Three models (MPM87, MPM93, and Ros98) showed a sharp change, from +2 to -2 K, when comparing 51.2 and 52.2 GHz channels with observations. At higher frequencies (55 – 60 GHz), they found the models were almost equivalent, but show a negative bias (~1 K) with respect to radiometric observations.

LILJEGREN et al.(2005) analysed 5 channels between 22 – 30 GHz and showed that using a 5% smaller width of the 22 GHz in Ros03 resulted in smaller bias in comparison with observed T_b, and also in retrieved profiles. Even temperature profiles above 3 km were improved by this modification, which is strange, as this information comes from the 51 – 52 GHz channels, which should not be sensitive to the width of this line. However it may be possible that the consistency between 20 – 30 and 51 – 53 GHz channels might improve the retrievals. Their results also suggested that replacing the Ros03 continuum with MT_CKD (MLAWER et al., 2003) improved the fit with T_b trends.

MATTIOLI et al.(2005) compared T_bs from 3 co-located Radiometrics instruments, each with channels at 23.8 and 31.4 GHz using 2 calibration algorithms, with Vaisala RS90 radiosonde measurements forward modelled with various absorption models. Their results supported the modification of the water vapour continuum in Lil05, but not the change in width of the 22 GHz line.

4. Dataset

This analysis uses observations from Payerne, Switzerland, (46.813° N, 6.943° E, 491 m altitude) in cloud free conditions during the Temperature Humidity and Cloud (TUC) experiment in winter 2003/04. See RUFFIEUX et al. (2006) and other papers in this issue for more details. The atmospheric conditions in the analysed dataset included many cases with temperature inversions and ranged in Integrated Water Vapour (IWV) from 3.1 to 18.7 kg/m^2 (mean = 7.7 kg/m^2) (MARTIN et al., 2006b). The surface temperatures ranged from -6.1 to +10.0 °C (mean = +1.4 °C). Only radiosondes launched in clear sky periods with good radiometer data were used in this validation exercise.

The instrumentation used is described below.

4.1. Radiometrics TP/WVP-3000

Radiometrics TP/WVP-3000 (WARE et al., 2003) is a ground-based microwave radiometer designed to allow retrieval of temperature and humidity profiles in the lower troposphere. It is normally configured to sample sequentially 5 channels in the water vapour band between 22.235 – 30 GHz and 7 channels along the edge of the oxygen complex between 51.25 – 58.8 GHz. All the channels are heterodyne, with double sidebands between ±(40 – 190) MHz of the nominal centre frequency. The effect of variable absorption across the channels' passbands is handled by defining an Effective Monochromatic Frequency (EMF), which corresponds to the single frequency that minimises the difference with the band-averaged absorption for a representative background dataset. As shown by CIMINI et al., (2006b), the EMF does not always correspond to the nominal central frequency. For the instruments and conditions experienced during the TUC experiment, the associated correction is less than 0.35 K for all channels.

The TP/WVP-3000 also incorporates an infrared radiometer to provide information on the cloud base.

During TUC, the Radiometrics TP/WVP-3000 was configured to view each of 7 zenith angles: 0°, ±60°, ±70°, ±75°, followed by a view of the ambient black body calibration target and an attempt to perform a tip curve calibration (HAN and WESTWATER, 2000) for the water vapour channels, viewing zenith+0°, ±45° and ±60°. For the first part of TUC (5/11/03 – 19/1/04), it was operated with v2.23 control software. This took ~300 s to complete the observing cycle. This was upgraded on 19/1/04 to v3.06, which reduced the observing cycle to 150 s, partially by omitting the tip curve calibrations. Instead constant calibration coefficients were calculated from data obtained while viewing a liquid nitrogen calibration target. Unfortunately, these were found to be inconsistent with earlier tip curve calibrations so only data from the water vapour channels obtained with v2.23 are used here.

4.2. ASMUWARA

The All-Sky MUlti WAvelength Radiometer (*ASMUWARA*) has 8 channels between 18 – 58 GHz and another at 151 GHz. It is described by MARTIN et al.(2006a). Throughout TUC, ASMUWARA was configured to perform continuous scans of 12 azimuth angles and 10 elevation angles. This sequence took approx. 21 min, including 12 zenith views. For its oxygen band channels, all azimuth angles were co-averaged to reduce the noise. However, during TUC these channels suffered a receiver problem, so only the water vapour channels and the highest frequency oxygen band channel is used here, as listed in Table 1.

4.3. Radiosondes

This study uses only the MeteoLabor SRS400 radiosondes launched from Payerne. These use carbon hygristors as humidity sensors, which are known to have a slow response time and poor accuracy, espe-

cially at low temperatures, but were also found to have a dry bias. Corrections were applied to the radiosondes' profiles based on comparisons with reference sondes with chilled-mirror hygrometers (RUFFIEUX et al., 2006). These corrections typically increased the Integrated Water Vapour by 5%.

5. Method

5.1. Profile selection

Only radiosondes launched in clear skies at times with valid radiometer data are analysed in this study. The following selection criteria were used:
– Radiometer data (not flagged as rain affected) available within 5 minutes of launch time
– Infrared T_b ≤-40°C
– Less than 2 oktas (eighths) of low and medium cloud cover observed at time of launch. (High cloud is allowed, as ice is not expected to contribute to the extinction at these frequencies.)
– Only the parts of the profile with valid humidity measurements were used (0<RH≤100%)

5.2. Profile top-up

The full vertical resolution of the radiosonde profiles (10 – 30 m) was used to define the levels between which layer averages were calculated for the radiative transfer. During TUC, the SRS400 typically only produced valid humidity measurements up to 10 – 12 km. Above this, the observed profile was 'topped-up' with a reference Mid-Latitude Winter profile. It was found that the choice of reference profile used for the top-up produced negligible differences to the modelled T_bs for the channels used in this study.

5.3. Radiative Transfer Calculations

In this study, brightness temperature, T_b, is defined to be linear with radiance, by applying a frequency dependent offset to the cosmic microwave background to account for departures from the Rayleigh-Jeans approximation, following JANSSEN (1993). These offsets are small at these frequencies – 0.04 K at 22.235 GHz increasing to 0.24 K at 58.8 GHz (but reaching 1.45 K at 151 GHz). Importantly, this is consistent with the definition of T_b used to calibrate both radiometers.

The down-welling radiance is integrated over each layer of the atmosphere at zenith angle, θ, following the discrete form of the Radiative Transfer Equation:

$$T_b\left(s_0,\theta\right)=T_b\left(s_1\right)e^{-\tau(s_1,\theta)}+\int_{s_0}^{s_1}\alpha\left(s\right)T\left(s\right).e^{-\tau(s,\theta)}ds$$

$$(1)$$

where $T_b(s_0,\theta)$ is the brightness temperature measured at zenith angle, θ. $T_b(s_1)$ is the brightness temperature of the background, s is the propagation path, $\alpha(s)$ is the absorption coefficient evaluated at the effective monochromatic frequency of each channel (CIMINI et al., 2006b), $T(s)$ is the physical temperature, and τ is the opacity, defined as:

$$\tau\left(s,\theta\right)=\int_{s_0}^{s}\alpha\left(s'\right)\sec\theta.ds'$$

$$(2)$$

6. Error Budget

In order to have confidence in the results of any validation exercise, it is necessary to conduct an error budget. Contributions to the random and systematic errors in T_b are assessed in this section. The total of the random errors are comparable to the scatter found in the resulting differences between modelled and observed T_bs. They are assumed to be negligible compared to the uncertainty on the systematic errors when averaged over 25 or more samples. The total uncertainty on the average T_b differences is dominated by the calibration accuracy of the radiometers and radiosondes. These figures are given in the right hand columns of Table 1 and the dotted lines in Figure 1.

6.1. Random Errors

Radiometric noise was evaluated as the variance of T_b measured while viewing a stable black body target over a period of 30 min – typically 0.1 – 0.2 K rms for integration times ~0.25 s. In fact, the random errors are usually dominated by the problems of representativeness in applying the radiosonde profile to the radiometers' observations.

6.2. Radiosonde Errors

The impact of systematic errors in the radiosonde profiles was estimated by study of the 7 triple flights on which 3 sensors were flown. The variance of T_b differences modelled by inputting these into the radiative transfer equation was used as a proxy for the error due to the sondes' sensors. These systematic errors introduce a 1-σ uncertainty of 0.2 K for channels dominated by oxygen absorption, and 0.5 K for channels near the 22 GHz water vapour line, shown in the column labelled 'Sonde Acc' in Table 1.

6.3. Radiometer Calibration Accuracy

The resulting biases should also be compared with the calibration accuracy of the radiometer observations. The accuracy of the Radiometrics TP/WVP-3000 was estimated by considering the uncertainty of

each term used in its calibration (HEWISON and GAFFARD, 2003). The column in Table 1 labelled 'MWR Acc' shows the resulting 1-σ accuracy is between 0.22 – 1.06 K. The calibration accuracy of ASMUWARA was estimated as 0.5 K for all channels, except 151 GHz (MARTIN et al., 2006a).

7. Results

Firstly the modelled T_bs were compared to those observed at time of the radiosondes' launch by both radiometers for zenith views only. The resulting differences for each sonde and model are shown in Figure 1. The average bias and root mean square difference of all available cases are summarised in Table 1 and Table 2, respectively.

The T_b differences were then studied for all zenith angles measured by the Radiometrics TP/WVP-3000, as shown in Figure 2. This extends the validation over a greater T_b range with consistent results. In this figure the same symbols are used for all zenith angles, so in most cases they are indistinguishable. However, different zenith angles can be identified by clusters of points, most obviously at 51.25 GHz. Here observations in opposite zenith angles show systematic differences (as much as 6 K) – probably due to misalignment of the instrument by ~0.5°. To reduce the influence of this, T_bs from angles on opposite sides of zenith are co-averaged. This reduces the uncertainty caused by instrument misalignment to <0.1 K.

7.1. Discussion of Results at 55 – 59 GHz

The highest frequencies (>55 GHz) of the Radiometrics TP/WVP-3000 show a consistent T_b bias of ~1 K. This is observed at all zenith angles. A similar bias was found previously in this instrument (HEWISON et al., 2003) and in another identical unit belonging to the Atmospheric Radiation Measurement (ARM) Program (CIMINI et al., 2004). All models agree here, and the expected error is small (~0.3 K). These results suggest this is likely to be a bias in the radiometer calibration. This is supported by the measurements of ASMUWARA's 57.2 GHz channel, and has subsequently been confirmed by simultaneous measurement with another radiometer (Radiometer Physics' HATPRO), operating at similar frequencies (ROSE et al., 2005). The manufacturers have identified the source of this error, which has been corrected in more recent control software. The T_bs of the 4 highest frequency channels of the Radiometrics TP/WVP-3000 have been corrected by applying constant corrections, based on the figures for Ros98. The corrected data have been used in all subsequent analysis presented in other papers in this issue.

7.2. Discussion of Results at 18 – 24 GHz

For the channels near the centre of the 22 GHz water vapour line, the observations generally agree with most models within the expected errors. However, ASMUWARA's 22.2 GHz channel appears to be inconsistent with the other results, suggesting it may be biased. Although both systems nominally have comparable calibration accuracies, their results differ by more than this. MPM93 consistently over-estimates the absorption in warmer, more humid conditions. There is also evidence of a temperature dependence on the MPM89 and Ros98 models, although the slope is not statistically significant.

At high zenith angles, large amounts of scatter are introduced to T_bs observed by the water vapour channels. This may be due to contamination of the antenna side-lobes by surface emission or atmospheric variability. However, when the highest zenith angles were omitted the scatter did not reduce much, but the slope reduced by ~1% at 22.235 GHz.

These results generally show smaller biases than previous analysis based on uncorrected RS80H radiosondes (HEWISON et al., 2003). This is partly due to the colder, drier conditions in the dataset and partly due to the correction of the radiosondes' humidity, which reduced the average bias in these channels by ~0.5 K. These results do not support the decreased width of the 22.235 GHz line in Lil05 (LILJEGREN et al., 2005), although this analysis is limited to winter conditions.

7.3. Results of water vapour continuum

In these winter conditions, the channels dominated by the water vapour continuum (26 – 30 GHz) show excellent agreement between the observations and all models except MPM93, which again overestimates the strength of the absorption. Note the consistent difference between the 2 radiometers, which was also observed by CIMINI et al. (2006b).

The same trend is even more pronounced at 151 GHz, although the noise on this channel is much larger. The slope of the regression lines are not significant for this channel. These results are consistent with those found in previous studies with this instrument (SCHNEEBELI, 2004), and an airborne radiometer at 157 GHz (HEWISON, 2005).

The modification of the water vapour continuum in Lil05 does not produce significantly different T_bs for most of the channels in this dataset, except at 151 GHz, where it slightly overestimates absorption compared to the observations and other models (except MPM93).

Table 1 - Average bias in zenith brightness temperatures observed during TUC for cases shown in Figure 1. Shading indicates level of bias significance with respect to the total systematic uncertainty, σ: Un-shaded: $0 \leq |\Delta T_b| < 1\sigma$, Light: $1\sigma \leq |\Delta T_b| < 2\sigma$, Mid: $2\sigma \leq |\Delta T_b| < 3\sigma$, Dark: $3\sigma \leq |\Delta T_b|$.

	Frequency	Average Bias Tb(model-obs) [K]						MWR	Sonde	Total
	[GHz]	MPM87	MPM89	MPM93	Ros98	Ros03	Lil05	Acc	Acc	σ
ASMUWARA	18.750	0.45	0.41	0.80	0.39	0.41	0.00	0.50	0.15	0.52
	22.200	2.32	1.94	2.81	1.86	1.92	2.81	0.50	0.51	0.71
	23.600	1.23	0.99	1.86	0.95	1.01	1.44	0.50	0.45	0.67
	31.500	0.31	-0.04	0.99	0.22	0.27	0.47	0.50	0.15	0.52
	57.200	-0.17	-0.19	-0.17	-0.18	-0.18	-0.18	0.50	0.18	0.53
	151.000	-0.98	-0.57	10.37	-2.00	-1.65	3.33	2.00	1.50	2.50
Radiometrics TP/WVP-3000	22.235	0.76	0.36	1.27	0.28	0.34	1.27	0.52	0.51	0.73
	23.035	0.81	0.48	1.40	0.42	0.48	1.18	0.40	0.50	0.64
	23.835	0.47	0.25	1.13	0.22	0.28	0.63	0.40	0.43	0.59
	26.235	0.36	0.19	1.01	0.27	0.31	0.37	0.29	0.24	0.38
	30.000	-0.01	-0.30	0.65	-0.10	-0.05	0.11	0.21	0.16	0.27
	51.250	-1.48	-0.22	-0.53	0.57	0.64	1.09	1.06	0.33	1.11
	52.280	0.21	1.90	0.97	2.60	2.66	3.02	0.89	0.28	0.93
	53.850	0.96	0.38	1.16	1.54	1.56	1.65	0.38	0.12	0.40
	54.940	-0.42	-0.71	-0.40	-0.43	-0.43	-0.42	0.24	0.14	0.28
	56.660	-0.97	-1.00	-0.97	-0.98	-0.98	-0.98	0.22	0.18	0.28
	57.290	-0.63	-0.64	-0.63	-0.64	-0.64	-0.64	0.22	0.18	0.28
	58.800	-0.70	-0.70	-0.70	-0.70	-0.70	-0.70	0.22	0.18	0.28

Table 2 – Root mean square difference between observed and modelled brightness temperatures for Figure 1. Shading indicates level of bias significance with respect to the total systematic uncertainty, σ: Un-shaded: $0 \leq |\Delta T_b| < 2\sigma$, Light: $2\sigma \leq |\Delta T_b| < 3\sigma$, Mid: $3\sigma \leq |\Delta T_b| < 4\sigma$, Dark: $4\sigma \leq |\Delta T_b|$.

|	Frequency	Root Mean Square Difference Tb(model-obs) [K]						MWR	Sonde	Total
	[GHz]	MPM87	MPM89	MPM93	Ros98	Ros03	Lil05	Acc	Acc	σ
ASMUWARA	18.750	0.59	0.56	0.91	0.54	0.56	0.58	0.50	0.15	0.52
	22.200	2.66	2.31	3.14	2.23	2.28	3.14	0.50	0.51	0.71
	23.600	1.60	1.42	2.17	1.38	1.42	1.78	0.50	0.45	0.67
	31.500	0.47	0.37	1.09	0.42	0.45	0.59	0.50	0.15	0.52
	57.200	0.29	0.30	0.29	0.29	0.29	0.29	0.50	0.18	0.53
	151.000	3.92	3.78	11.48	4.24	4.09	5.22	2.00	1.50	2.50
Radiometrics TP/WVP-3000	22.235	1.36	1.17	1.73	1.15	1.16	1.73	0.52	0.51	0.73
	23.035	1.31	1.14	1.77	1.11	1.14	1.59	0.40	0.50	0.64
	23.835	0.95	0.86	1.44	0.84	0.86	1.04	0.40	0.43	0.59
	26.235	0.58	0.50	1.14	0.53	0.55	0.59	0.29	0.24	0.38
	30.000	0.54	0.63	0.91	0.55	0.54	0.55	0.21	0.16	0.27
	51.250	1.61	0.59	0.87	0.86	0.91	1.27	1.06	0.33	1.11
	52.280	0.76	2.00	1.21	2.70	2.76	3.10	0.89	0.28	0.93
	53.850	1.10	0.62	1.27	1.64	1.65	1.74	0.38	0.12	0.40
	54.940	0.60	0.83	0.59	0.61	0.61	0.60	0.24	0.14	0.28
	56.660	1.05	1.07	1.05	1.06	1.06	1.06	0.22	0.18	0.28
	57.290	0.80	0.81	0.80	0.81	0.81	0.81	0.22	0.18	0.28
	58.800	0.77	0.77	0.77	0.77	0.77	0.77	0.22	0.18	0.28
Average	WV Line	1.78	1.54	2.21	1.49	1.53	2.15	0.47	0.51	0.70
	WV Cont	1.24	1.16	2.74	1.21	1.21	1.48	0.63	0.44	0.78
	Oxygen	0.87	0.88	0.86	1.09	1.11	1.20	0.47	0.20	0.51
	All	1.30	1.19	1.93	1.27	1.28	1.61	0.52	0.38	0.66
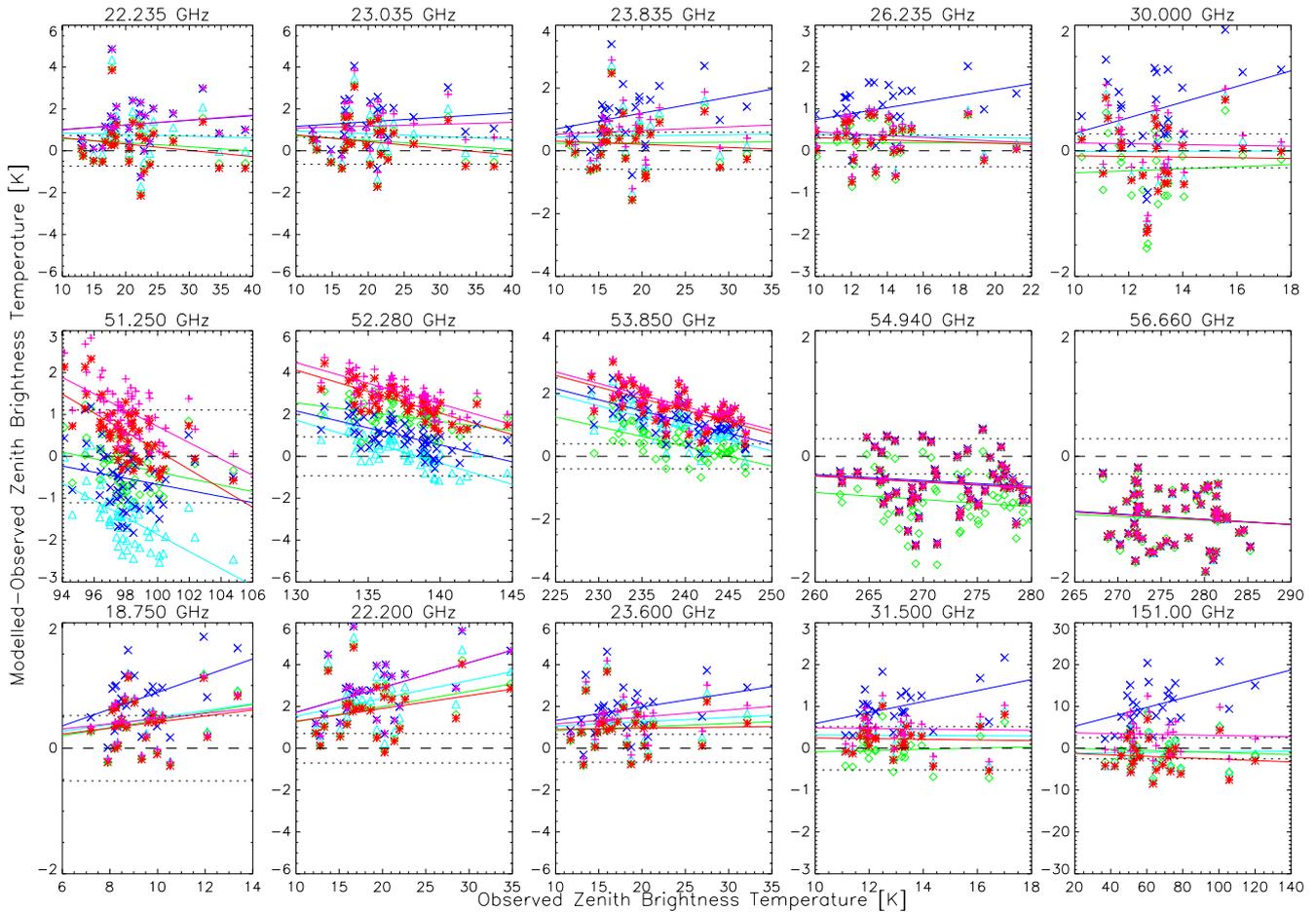
Figure 1 – Modelled-Observed zenith brightness temperatures during TUC experiment in Payerne.
Each point is 1 radiosonde, modelled using MPM87(Δ), MPM89(◊), MPM93(x), Ros98(∗), Lil05(+).
Solid lines show the linear regression through all point for each model (same colour).
Top row is Radiometrics TP/WVP-3000 water vapour channels with 27 cases (5/11/03-20/1/04).
Middle row is first 5 Radiometrics TP/WVP-3000 oxygen band channels with 54 cases (5/11/03-14/2/04).
Bottom row is ASMUWARA water vapour channels with 25 cases (5/11/03-20/1/04).
Dotted lines show total 1-σ uncertainty of average T_b difference including accuracy of radiometer and radiosonde.
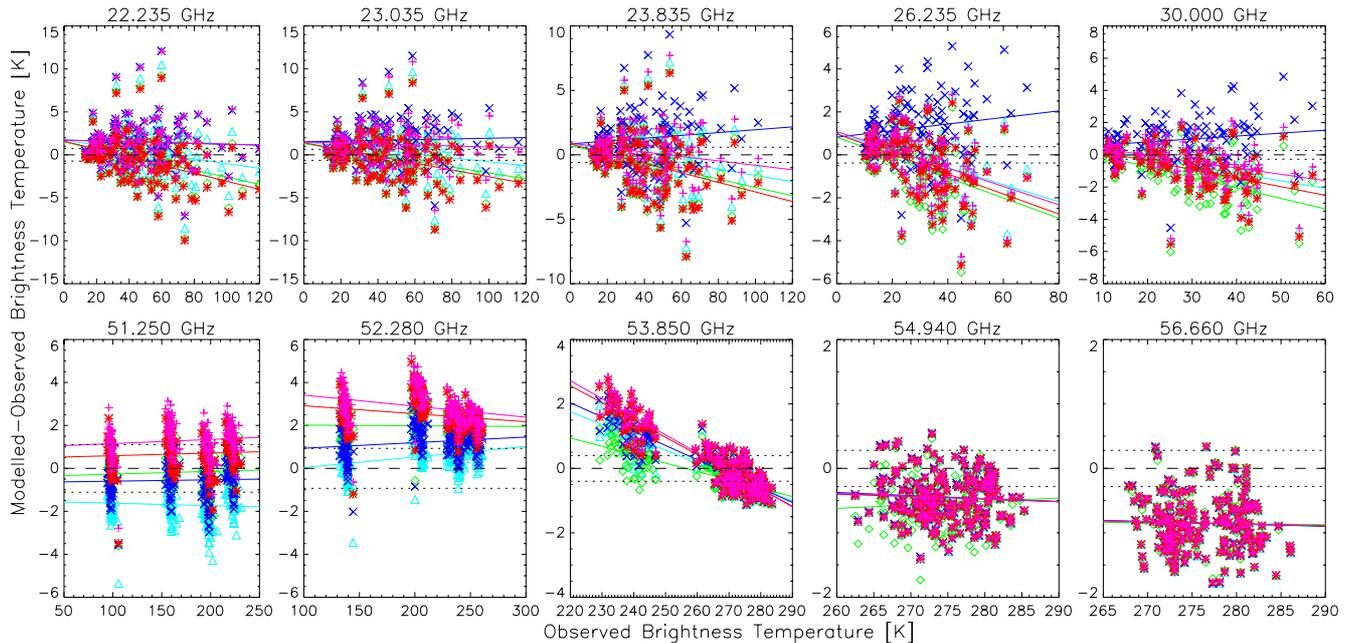

Figure 2 – As Figure 1, but for all Radiometrics TP/WVP-3000 zenith angles: 0°, ±60°, ±70° and ±75°.

7.4. Discussion of Results at 51 – 55 GHz

The water vapour continuum also influences the channels on the edge of the oxygen band (51 – 52 GHz). These channels (also 53.85 GHz) show the largest difference between the models and significant differences between the observations and models. These channels are also most difficult to calibrate accurately. Their response is complex as it combines the influence of water vapour continuum and oxygen line coupling parameters, both of which change between the different models. To help understand the cause of the bias observed here, it is helpful to also consider the response at other zenith angles, shown in Figure 2.

At 51.25 GHz, MPM89 and MPM93 provide the closest match to the observations at both zenith and other angles, while Ros98 and Lil05 overestimate the emission at low temperatures and at lower elevation angles, and MPM87 underestimates in warmer conditions and at higher zenith angles.

However, the pattern changes at 52.28 GHz, where all models show a significant temperature dependence, and only MPM87 does not significantly overestimate the emission.

By 53.85 GHz, the atmosphere becomes optically thick at high temperatures and zenith angles and all models again converge, presumably to approach the same bias observed at higher frequencies. In cold conditions at zenith, MPM89 provides the best fit to the observations, but all models again overestimate the emission.

BOUKABARA et al. (2005) showed the modelled absorption at 50 – 53 GHz is critically dependent on the assumptions made about the strength of the oxygen line coupling values used in the models. These were derived from lab measurements between +6 to +54°C and have been extrapolated to apply at lower temperatures found near the surface in this dataset and throughout the upper troposphere and stratosphere. The apparent temperature dependent bias found here in these channels would support an error of this type. However it is beyond the scope of this paper to investigate how oxygen line coupling may be adjusted. The difficulty in calibrating these channels in a ground-based microwave radiometer will hamper further investigation. This suggests that this aspect of the spectroscopy would benefit from further lab measurements at lower temperatures.

7.5. Inter-channel Correlations

It can also be instructive to study the correlations and differences between channels. Not only can this highlight inconsistencies between observations and models at different frequencies, but also it closely resembles how observation/model error can manifest in the retrieval process.

Figure 3 shows the difference in zenith T_b between selected channels plotted against T_b of the lower frequency channel of the pair. The points in each panel show the observed and modelled T_b of each radiosonde in clear air. Observations and different models are shown by different symbols and colours, according to the legend. The solid lines show the linear regression through the data of the corresponding colour.

The slope of the lines in Figure 3 shows the relative consistency of the models with the observations. Calibration biases can cause the offsets to vary, although the T_b difference of similar channels is less sensitive to calibration bias than the absolute T_b.

There is very little difference in slope between the Liebe/Rosenkranz models near 22.235 GHz, and all provide a reasonable fit to the observed slope. However, Lil05 tends to overestimate the slope here, while it is closer to the observed slope between 23.835 – 23.035 GHz.

Most models (except MPM93) are consistent with the observations for the channels dominated by the water vapour continuum, although Lil05 is closest for 151 – 31.5 GHz.

The slopes of the channels on the edge of the oxygen band at 51 – 54 GHz are much more variable between the different models. Generally, MPM89 is most consistent with the observations here, although the 54/55 GHz pair is anomalous. This pair spans the range over which T_b saturates as the atmosphere becomes optically thick. The differences were small at higher frequencies in the oxygen band (not shown).
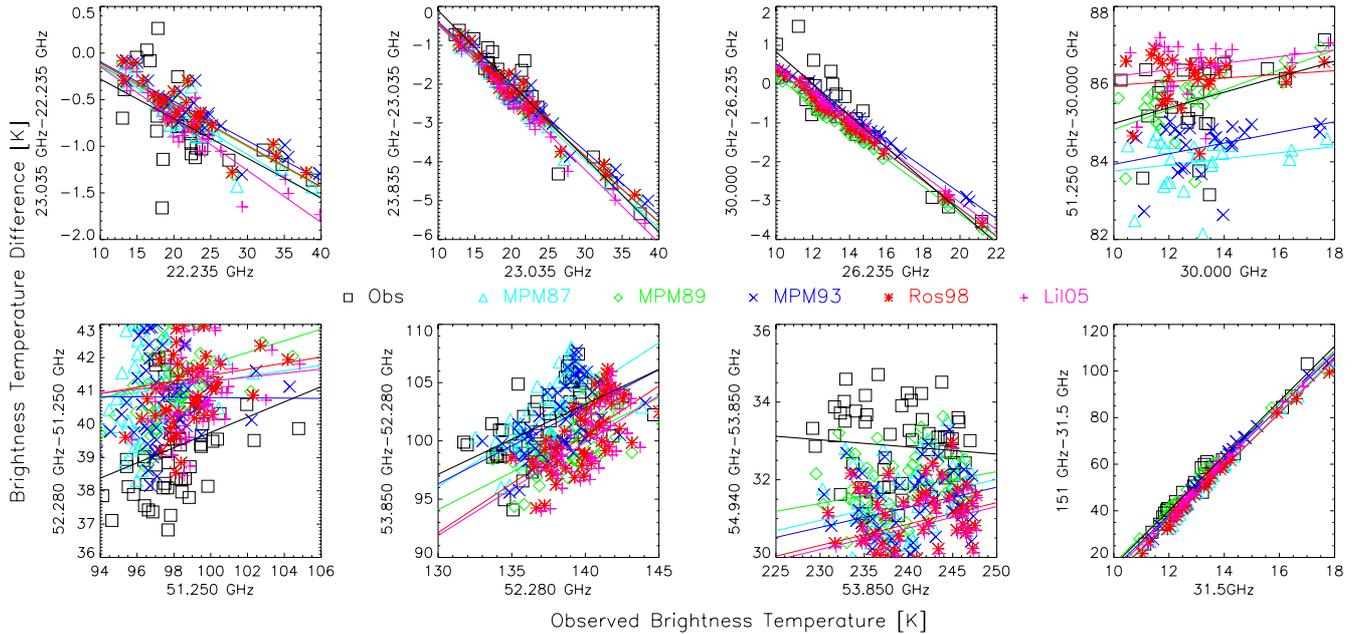
Figure 3 - Observed and modelled T_b difference between adjacent channels during TUC in clear sky.
Observed (□) and modelled by MPM87(Δ), MPM89(◊), MPM93(x), Ros98(∗), Lil05(+).
Lines indicate linear regression fitted through data.

8. Conclusions

This study has compared the modelled brightness temperatures from radiosondes launched in clear skies during TUC with observations from 2 ground-based microwave radiometers. It is important to understand the resulting biases as they impact on the accuracy of any retrievals from these instruments which use the absorption models. Validation studies such as this can form an important part of the development cycle of new observations and define the uncertainty in observations and models, needed for optimal retrievals from them.

Overall, MPM89 provided the best fit to the observations used in this study, in terms of average bias and rms difference, although Ros98 offered small improvements near the 22.235 GHz water vapour line, as MPM93 did in the oxygen band at 51 – 59 GHz. However, MPM93 was found to be consistently biased in the water vapour continuum.

A bias was found in the calibration of the oxygen band channels of the Radiometrics TP/WVP-3000, most obviously at 55 – 59 GHz. This bias has been empirically corrected in the TUC dataset for subsequent analysis. The cause of this bias has now been identified and corrected by the manufacturers.

The results for channels in the water vapour band are also sensitive to the accuracy of the radiosonde humidity profiles. The known dry bias of the Vaisala RS80 radiosondes explains the difference between our results for 22 – 30 GHz and those reported from an-

other dataset with the same instrument (HEWISON et al., 2003) using these radiosondes. Their results for the other channels were consistent with ours.

These results do not support the modifications of the width of the 22.235 GHz water vapour line or continuum proposed by LILJEGREN et al. (2005), although they are based on only winter-time data. However, this conclusion is critically dependent on the accuracy of the radiosonde humidity sensors, which are not known to better than 3 – 5 %. Similar conclusions were reported by MATTIOLI et al.(2005).

The conclusions of CIMINI et al. (2004) are broadly consistent with our results, although they were based on observations in mid-latitude summer conditions. However, the bias we found in 51 – 52 GHz channels for the TUC data depends on the conditions: the models tend to predict too much absorption in cold/dry conditions, but too little in warmer conditions. This temperature-dependent bias may be explained as an error in the oxygen line coupling parameters, as shown by BOUKABARA et al. (2005). However, it is difficult to identify possible corrections with the existing dataset, which, like similar attempts, are limited by radiometer calibration and radiosonde accuracy. Further laboratory measurements of oxygen absorption in this band at low temperatures are needed to improve this.

References

BOUKABARA, S.A., S.A.CLOUGH, J-L MONCET, A.F.KRUPNOV, M.TRETYAKOV and V.V.PARSHIN, 2005: Uncertainties in the Temperature Dependence of the Line Coupling Parameters of the Microwave Oxygen Band: Impact Study, IEEE Trans. Geosci. Rem. Sensing, Vol.43, No.5.

CIMINI, C., F.S.MARZANO, P.CIOTTI, Y.HAN, D.CIMINI, S.J.KEIHM, E.R.WESTWATER, R.WARE, 2004: Atmospheric Microwave Radiative Models Study Based on Ground-Based Multichannel Radiometer Observations in the 20-60 GHz Band, Fourteenth ARM Science Team Meeting Proceedings, Albuquerque, New Mexico, March 22-26, 2004

CIMINI, D., T.J.HEWISON, L. MARTIN, J.GUELDNER, C.GAFFARD F. MARZANO, , 2006a: Temperature and Humidity profile retrievals from ground-based microwave radiometers during TUC, Meteorol. Z., This issue.

CIMINI, D., T.J. HEWISON, L. MARTIN, 2006b: Comparison of brightness temperatures observed from ground-based microwave radiometers during TUC, Meteorol. Z., This issue.

HAN, Y. and E.R.WESTWATER, 2000: Analysis And Improvement Of Tipping Calibration For Ground-Based Microwave Radiometers, IEEE Trans. Geosci. Rem. Sens., Vol.38, No.3, pp.1260-1276.

HEWISON, T.J. and C.GAFFARD, 2003: Radiometrics MP3008 Microwave Radiometer Trial Report, Met Office (OD) Technical Report 26, Available from National Meteorological Library, UK.

HEWISON, T.J., C.GAFFARD and J.NASH, 2003: Validation of Microwave Radiometer Measurements in Clear Air, ISTP conference, Leipzig, Germany.

HEWISON, T.J., 2005: Aircraft Validation of Clear Air Absorption Models at Millimetre Wavelengths (89-183 GHz), Submitted to Journal of Geophysical Research, 2005.

JANSSEN, M., 1993: Atmospheric Remote Sensing by Microwave Radiometry, Wiley Series in Remote Sensing, pp.318.

LIEBE, H.J and D.H.LAYTON, 1987: Millimeter-Wave Properties Of The Atmosphere: Laboratory Studies And Propagation Modeling, NTIA-Report 87-224, Natl. Telecommun. And Inf. Admin, Boulder, CO.

LIEBE, H.J., 1989: MPM - An Atmospheric Millimeter Wave Propagation Model, Int. J. Infrared and Millimeter Waves, Vol.10(6), pp.631-650.

LIEBE, H.J., G.A.HUFFORD and M.G.COTTON, 1993: Propagation modeling of moist air and suspended water/ice particles at frequencies below 1000GHz, AGARD 52nd Specialists' Meeting of the Electromagnetic Wave Propagation Panel, Ch3.

LILJEGREN, J.C., S.A.BOUKABARA, K.CADY-PEREIRA and S.A.CLOUGH, 2005: The Effect of the Half-Width of the 22-GHz Water Vapor Line on Retrievals of Temperature and Water Vapor Profiles with a Twelve-Channel Microwave Radiometer, IEEE Trans. Geosc. Rem. Sens., Vol.43, No.5, pp.1102-1108.

MARTIN, L., M.SCHNEEBELI, and C.MÄTZLER, 2006a: ASMUWARA, a ground-based radiometer system for tropospheric monitoring, Meterol. Z., This issue.

MARTIN, L. C.MÄTZLER, T.HEWISON and D.RUFFIEUX, 2006b: Intercomparison of integrated water vapour measurements during the TUC Campaign, Meterol. Z., This issue.

MATTIOLI, V., E. WESTWATER, S. GUTMAN and V. MORRIS, 2005: Forward Model Studies of Water Vapor using Scanning Microwave Radiometers, Global Positioning System, and Radiosondes during the Cloudiness Inter-Comparison Experiment, IEEE Trans. Geosci. Rem. Sens., Vol.43, No.5, pp.1012-1021.

MLAWER, E. J., S.A.CLOUGH AND D.C.TOBIN, 2003: The MT_CKD water vapour continuum: A revised perspective including collision induced effects, presented at the Atmospheric Science from Space using Fourier Transform Spectrometry (ASSFTS) Workshop, Bad Wildbad, Germany, 8-10 October 2003.

ROSE, T., S.CREWELL, U.LÖHNERT and C.SIMMER, 2005: A network suitable microwave radiometer for operational monitoring of the cloudy atmosphere, Atmospheric Research, Vol. 75, Issue 3 , May 2005, pp.183-200.

ROSENKRANZ, P.W., 1998: Water Vapor Microwave Continuum Absorption: A Comparison Of Measurements And Models, Radio Science, Vol.33, No.4, pp.919-928 and correction in Radio Science, Vol.34, No.4, p.1025, 1999.

RUFFIEUX, D., J.NASH, P.JEANNET and J.AGNEW, 2006: The COST720 Temperature, Humidity and Cloud Profiling Campaign: TUC, Meterol. Z., This issue.

SCHNEEBELI, M., 2004: Modellierung und Messung von Mikrowellen- und Infrarotstrahlung durch klare und bewölkte Atmosphären, Master Thesis, Philosophisch-Naturwissenschaftliche Fakultät, Universität Bern, Switzerland.

WARE, R., F. SOLHEIM, R. CARPENTER, J. GUELDNER, J. LILJEGREN, T. NEHRKORN, F. VANDENBERGHE, 2003: A multi-channel radiometric profiler of temperature, humidity and cloud liquid, Radio Science 38, 8079, doi:10.1029/2002RS002856.